AD-A145 795 ICING RATE ON STATIONARY STRUCTURES UNDER MARINE CONDITIONS(U) COLD REGIONS RESEARCH AND ENGINEERING LAB HANOVER NH K ITAGAKI JUN 84 CRREL-84-12 1/1

UNCLASSIFIED F/G 4/2 NL

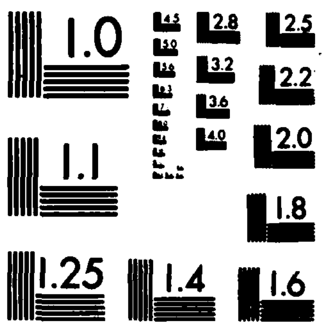

MICROCOPY RESOLUTION TEST CHART
NATIONAL BUREAU OF STANDARDS-1963-A

CRREL REPORT 84-12

US Army Corps of Engineers
Cold Regions Research & Engineering Laboratory

Icing rate on stationary structures under marine conditions

For conversion of SI metric units to U.S./British customary units of measurement consult ASTM Standard E380, Metric Practice Guide, *published by the American Society for Testing and Materials, 1916 Race St., Philadelphia, Pa. 19103.*

Cover: Sea spray icing developed during a winter storm in the Baltic Sea between Sweden and Finland. Photo courtesy of L. Makkonen.

12

CRREL Report 84-12

June 1984

Icing rate on stationary structures under marine conditions

Kazuhiko Itagaki

Prepared for
OFFICE OF THE CHIEF OF ENGINEERS
Approved for public release; distribution is unlimited

Unclassified

SECURITY CLASSIFICATION OF THIS PAGE *(When Data Entered)*

REPORT DOCUMENTATION PAGE		READ INSTRUCTIONS BEFORE COMPLETING FORM
1. REPORT NUMBER CRREL Report 84-12	2. GOVT ACCESSION NO.	3. RECIPIENT'S CATALOG NUMBER
4. TITLE *(and Subtitle)* ICING RATE ON STATIONARY STRUCTURES UNDER MARINE CONDITIONS		5. TYPE OF REPORT & PERIOD COVERED
		6. PERFORMING ORG. REPORT NUMBER
7. AUTHOR(s) Kazuhiko Itagaki		8. CONTRACT OR GRANT NUMBER(s)
9. PERFORMING ORGANIZATION NAME AND ADDRESS U.S. Army Cold Regions Research and Engineering Laboratory Hanover, New Hampshire 03755		10. PROGRAM ELEMENT, PROJECT, TASK AREA & WORK UNIT NUMBERS DA Project 4A161102AT24, Task C, Technical Effort El, Work Unit 002
11. CONTROLLING OFFICE NAME AND ADDRESS Office of the Chief of Engineers Washington, DC 02314		12. REPORT DATE June 1984
		13. NUMBER OF PAGES 13
14. MONITORING AGENCY NAME & ADDRESS *(if different from Controlling Office)*		15. SECURITY CLASS. *(of this report)* Unclassified
		15a. DECLASSIFICATION/DOWNGRADING SCHEDULE

16. DISTRIBUTION STATEMENT *(of this Report)*

Approved for public release; distribution unlimited.

17. DISTRIBUTION STATEMENT *(of the abstract entered in Block 20, if different from Report)*

18. SUPPLEMENTARY NOTES

19. KEY WORDS *(Continue on reverse side if necessary and identify by block number)*

Icing
Ice formation
Offshore drilling
Offshore structures
Ships
Ship icing

20. ABSTRACT *(Continue on reverse side if necessary and identify by block number)*

The rate of ice accumulation on stationary structures was calculated using published data. The results were compared with icing measured on board ships. Although the general trend of this calculation indicated parallelism with the on-board measurements, the measured ice accumulation rate on ships needed a 5 to 8 m/s higher windspeed to correspond with the calculated rate for stationary structures.

DD FORM 1 JAN 73 1473 EDITION OF 1 NOV 65 IS OBSOLETE

Unclassified

SECURITY CLASSIFICATION OF THIS PAGE *(When Data Entered)*

PREFACE

This report was prepared by Dr. Kazuhiko Itagaki, Research Physicist, Snow and Ice Branch, Research Division, U.S. Army Cold Regions Research and Engineering Laboratory. Funding was provided by DA Project 4A161102AT24, *Research in Snow, Ice and Frozen Ground*; Task C, *Research in Terrain and Climatic Constraints Environment*; Technical Effort E1, *Cold Environment Factors*; Work Unit 002, *Adhesion and Physics of Ice.*

Technical review was provided by Stephen Ackley, Chief of the Snow and Ice Branch, and Dr. Motoi Kumai, CRREL.

A1

ICING RATE ON STATIONARY STRUCTURES UNDER MARINE CONDITIONS

Kazuhiko Itagaki

INTRODUCTION

Icing on stationary structures such as oil rigs is becoming an increasingly serious problem as offshore drilling operations in the subpolar regions become more common. ~~Very little, if any,~~ information exists on this subject. Extensive observations have been made of icing on the upper structures of moving ships, but the complexity of this problem makes analysis of the results very difficult. Even the generation of water drops in this case involves many factors, such as windspeed, wave direction relative to the bearing of the ship, and size and freeboard of the ship. On stationary structures, however, the problem is much simpler, since the major factor in drop generation is whitecaps produced by wind, and no motion of the structure is involved.

In the present study, a theoretical calculation was made by combining the data available on the generation of drops by wind with data on the proportion of ice frozen from the collected water. Although the results discussed in this paper are preliminary and a wider range of reliable data is required, the general trend of the calculations for stationary structures is surprisingly parallel with observations made on board ships.

PROPORTION OF SEA SPRAY FROZEN ON THE STRUCTURE

The rate of ice accumulation R can be calculated by the following formula:

$$R = C_f C_c F \tag{1}$$

where F is mass flux of the water drops and C_f and C_c are the proportions of spray frozen on the surface (freezing factor) and the coefficient of capture of drops respectively. C_c can be close to unity for larger drops such as sea spray. Although many other factors may contribute, C_f seems to be a strong function of the air temperature. The relationship between mean air temperature and freezing factor (frozen mass/captured mass) obtained from data given by Ono (1964), and reproduced in Table 1, indicates that C_f increases linearly as the air temperature decreases, as shown in Figure 1.

Table 1. Amounts and chlorinities of accumulated brine (after Ono 1964).
Parentheses indicate calculated values assuming chlorinity of respective value of sea spray (19‰).

Date and time	Ice Weight (g)	Ice Chlorinity (0/00)	Brine Weight (g)	Brine Chlorinity (0/00)	Accumulation rate Ice (g/hr)	Accumulation rate Brine (g/hr)	Accumulation rate Sea spray (g/hr)	Chlorinity of sea spray (0/00)	Freezing factor C_f (% ice)	Mean air temp. (°C)	Mean water temp. (°C)	Mean rel. wind speed (m/s)
Results from icing gauge, 1962												
15 January												
1345-1600	35	—	10	—	15.6	4.4	20.0	—	78	- 5.8	2.0	9.0
1600-2000	90	15.1	20	32.0	22.5	5.0	27.5	18.2	82	- 6.6	1.4	11.6
2000-0000	105	13.2	(890)	(19.6)	26.3	(222.5)	(248.8)	(19.0)	11*	- 6.6	0.1	15.6
16 January												
0000-0400	304	14.5	190	29.0	85.0	47.5	132.5	19.7	64	- 9.8	-0.9	15.5
0400-0700	5	—	0	—	1.7	0	1.7	—	100	-12.6	-1.3	13.1
1400-1600	30	16.7	0	—	15.0	0	15.0	—	100	-11.4	-0.8	10.3
1600-1810	95	16.0	10	36.4	43.8	4.6	48.4	18.0	90	-12.7	-1.0	11.3
17 January												
0200-0400	390	—	270	—	195.0	135.0	330.0	—	59	- 7.2	0.5	15.4
0400-0710	335	(10.4)	410	26.0	105.7	129.3	235.0	(19.0)	45	- 6.9	1.5	12.2
Results from icing gauge, 1963												
9 January												
1540-2200	49.4	11.5	(773)	19.6	7.5	(117.1)	(124.6)	(19.1)	6	- 1.0	1.5	10.5
2200-0000	52.4	6.3	212.2	22.1	26.2	106.1	132.3	19.1	20	- 2.0	-0.4	9.7
10 January												
0000-0400	72.3	5.9	(329)	22.0	18.1	(82.2)	(100.3)	(19.1)	18	- 2.0	-0.1	10.2
0400-1200	439.0	8.7	(977)	24.0	54.9	(122.1)	(177.0)	(19.1)	31	- 3.5	2.4	12.0
1200-1600	356.4	8.9	(634)	25.1	89.1	(158.5)	(247.6)	(19.1)	36	- 5.7	1.0	15.5

* Washed by large amount of seawater.

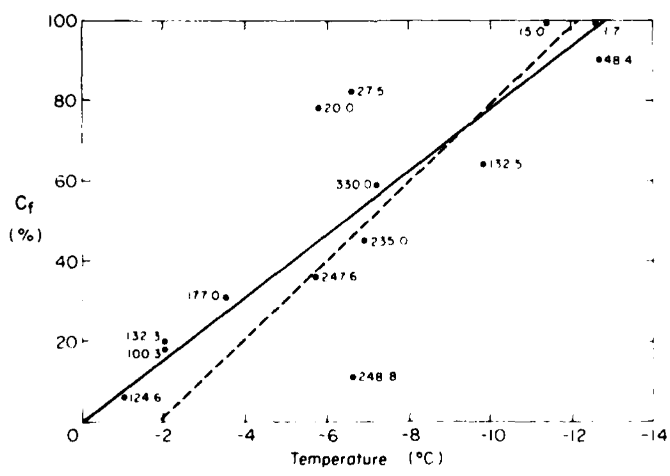

Figure 1. Freezing factor as a function of air temperature using data of Ono (1964). Numbers next to the data points indicate the amount of sea spray collected by the icing gauge (g/hr). Solid line is simpler regression equation.

Table 2. Temperature versus freezing factor.

Air temperature (°C)	Freezing factor, C_f
- 2.000	0.155
- 4.000	0.311
- 6.000	0.466
- 8.000	0.621
-10.000	0.777
-12.000	0.932
-12.878	1.000

The linear regression analysis of the air temperature versus C_f indicates that the regression line intersects the x-axis at 0.48 °C. The x-intercept is expected to be between 0.C° and the freezing point of seawater (-1.9 °C) unless the air is very dry. The wide scatter in the data points may be the major source of the discrepancy in the regression line intercept. C_f may also be a function of the mass flux F, making the data points more widely scattered. In addition, a possible nonlinearity in temperature versus C_f was disregarded for the regression analysis. Since data points were scattered so widely, the simpler form

$$C_f = 0.07765\ T \tag{2}$$

was used instead of the more complex equation, bringing the x-intercept to 0.48 °C.

This regression line is shown as the solid line in Figure 1. By use of eq 2, C_f becomes unity at -12.878 °C (T_l), but again this temperature could be considerably higher than the actual case. Brine pockets in sea ice freeze at about -18 °C, limiting the lowest temperature. Brine drains out faster from the accreted ice than from sea ice because of its porous structure; therefore, T_l for brine would not be as low as that for sea ice. More accurate data are needed to clear up these points. The calculated C_f values as a function of temperature are shown in Table 2.

MASS FLUX

Mass flux can be written as

$$F = \frac{4\pi\varrho}{3} \int n(r) V\, r^3 dr = \frac{4\pi}{3 \cdot 8}\, \varrho \int n(\phi)\ V \phi^3 d\phi \tag{3}$$

where $n(r)$ is the number of drops of radius r (diameter ϕ) in unit volume, V is the wind velocity and ϱ is the density of water. $n(r)$ is a function of wind velocity and height of observation. In icing of a ship, the mass flux is a comglex function of the wave direction and height, the wind direction and velocity, the ship's bearing and speed, and the overall structure and size of the ship. In icing of a stationary structure, the mass flux at a fixed height is primarily dependent upon the windspeed.

Lai and Shemdin (1974) compiled some data from other researchers (Toba 1961, Monahan 1968) together with their own data on the size distribution of sea spray in their Figure 12 (reproduced and shown in Fig. 2 here). Generally, the distribution of the number density is inversely proportional to the square of the drop diameter ϕ, as

$$n(\phi, V) = \frac{A(V)}{\phi^2} \tag{4}$$

where the constants $A(V)$ were determined for each windspeed plot for a diameter of $\phi = 10^{-1}$ cm (listed in Table 3).

These constants $A(V)$ were adjusted for a height of 13 cm from the average water surface for the extrapolated windspeed at 10 m from the water surface in the original figure of Lai and Shemdin (1974). The mass flux F was then

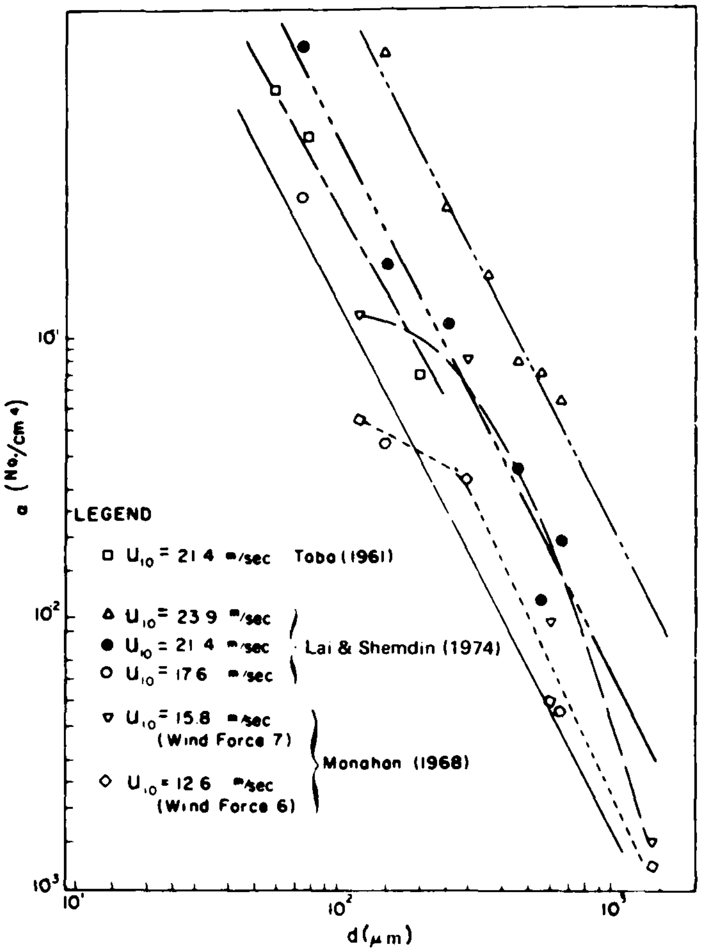

Figure 2. Size distribution of sea spray [from Lai and Shemdin, Journal of Geophysical Research, *79(21): 3055–3063, 1974; copyrighted by the American Geophysical Union].*

$$F = \frac{4\pi}{3\cdot 8}\varrho V A(V) \int \frac{\phi^3}{\phi^2} d\phi. \tag{5}$$

Since the drop diameters observed by Lai and Shemdin (1974) were between 50 and 700 μm, integration in this domain yielded F as

$$F = -\frac{\pi}{12}\varrho V A(V)\left[(7\times 10^{-4})^2 - (5\times 10^{-5})^2\right] \text{ kg/m}^2\text{s}. \tag{6}$$

Table 3. A(V) and windspeed versus mass flux, calculated from Lai and Shemdin (1974).

Wind (m/s)	*A(V) at 1 mm (no./m³)*	*Mass flux (kg/m²s)*
12.6	2.0×10^{-1}	3.21×10^{-4}
15.8	4.5	9.07
16.4	5.9	12.35
18.9	24.0	57.89

The experimental data points of Lai and Shemdin and of Toba seemed systematically deviated from the field data points of Monahan for a windspeed that is 5 m/s lower. Therefore, all the experimental data points for windspeed were shifted 5 m/s lower to maintain consistency of the results.

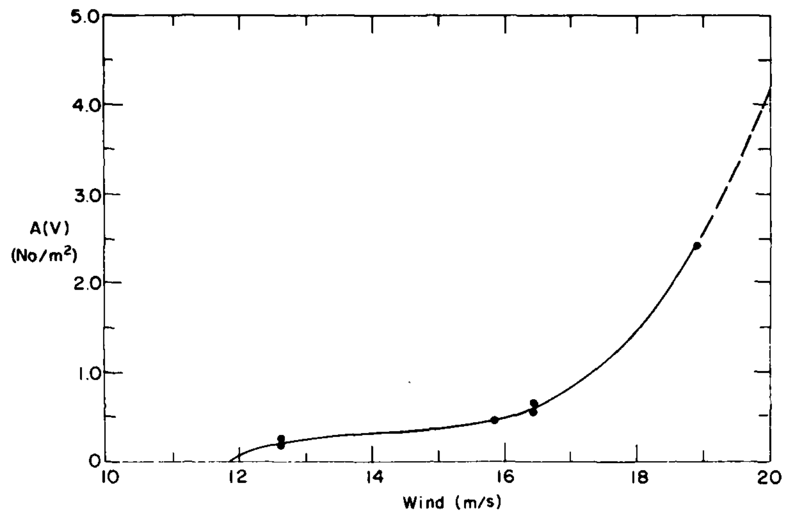

Figure 3. Proportional factor of number density A(V) *as a function of windspeed.*

A third-degree polynomial regression fitted the relationship between windspeed V and $A(V)$ fairly well (Fig. 3):

$$A(V) = A_0 + A_1 V + A_2 V^2 + A_3 V^3 \tag{7}$$

where the constants were $A_0 = -53.5173$, $A_1 = 11.3119$, $A_2 = -0.7943$ and $A_3 = 0.01864$.

Mass flux F was calculated and is shown in Table 3 for the corresponding windspeed.

ICE ACCRETION RATE

The ice accretion rates R, calculated from the above data using eq 1, are shown in Table 4 at 2°C intervals, using a capture coefficient C_c of 1.

In order to obtain the semi-empirical relationship between temperature T and windspeed V for a fixed ice accumulation rate R, eq 2, 6 and 7 were combined into eq 1 and solved for T:

$$T = \frac{A_4 R}{VA_0 + V^2 A_1 + V^3 A_2 + V^4 A_3} \tag{8}$$

where A_0–A_3 are the same as in eq 7 and $A_4 = 12.8781$. The results are shown in Figure 4 with R as a parameter. Since the flux was calculated from values observed near the sea surface (13 cm above the surface), direct comparison with ship icing data obtained from onboard observations is difficult. However, the general trend showed surprisingly good parallelism with the diagrams given by previous authors.

DISCUSSION

The icing rates measured onboard ships by Ono (1964), using an icing gauge (collecting cross section of 2.2 by 14.5 cm), are shown by dots in Figure 4. The rates were converted into kg/m² hr and are shown by the numbers next to the data points. It is difficult to compare

Table 4. Calculated ice accretion rate.

Wind (m/s)	Air temperature (°C)	Ice accretion rate R (kg/m²hr)	Wind (m/s)	Air temperature (°C)	Ice accretion rate R (kg/m²hr)
12.6	- 2.000	0.180	16.4	- 2.000	0.690
	- 4.000	0.360		- 4.000	1.381
	- 6.000	0.539		- 6.000	2.071
	- 8.000	0.719		- 8.000	2.762
	-10.000	0.899		-10.000	3.452
	-12.000	1.079		-12.000	4.143
	-12.878	1.158		-12.878	4.446
15.8	- 2.000	0.507	18.9	- 2.000	3.237
	- 4.000	1.015		- 4.000	6.473
	- 6.000	1.522		- 6.000	9.710
	- 8.000	2.029		- 8.000	12.947
	-10.000	2.537		-10.000	16.183
	-12.000	3.044		-12.000	19.420
	-12.878	3.267		-12.878	20.841

these points directly with the calculated values because the major mechanism of sea spray generation in Ono's case is not the wind but rather the pounding of the waves against the ship's hull. Generally, the observed icing rates found by Ono correspond to the calculated value in Figure 4 at 5 to 8 m/s higher windspeeds.

Figure 5, from Tabata (1966), depicts the relationship of the icing class to the temperature and relative windspeed for 350-ton and 450-ton class cutters. It is clear that increasingly higher windspeed is required to produce considerable icing above -5 °C, while little temperature effect is seen below -5 °C. The same trend can be seen in Figure 4, although a much higher windspeed is needed for the *stationary* structure to produce similar icing rates.

Total ice accumulation rate was measured on a Japanese cutter by Tabata et al. (1963) and correlated with air temperature and Beaufort wind scale as shown in Figure 6. The area of ice coverage was roughly 150 m² and the maximum accumulation rate at Beaufort wind scale 5 and -7 °C was 13 kg/m² hr (1.99 tons/hr), which corresponds to a windspeed of 19 m/s or Beaufort 8 in the present calculation. The maximum accretion rate obtained by the icing gauge (Ono 1964) was 61 kg/m² hr for -7 °C and 15.4 m/s, which is again at least one order of magnitude larger than in the present calculation. The difference in the spray production mechanism on ships compared with that on stationary structures may account for the difference in icing rates.

The mass flux observed under laboratory conditions (Toba 1961, Lai and Shemdin 1974) corresponded to that under natural conditions (Monahan 1968) with a windspeed of 5 m/s less. Two major reasons possibly contributed to this discrepancy. First, the vast, open windward water (fetch) creates roughness considerably higher than laboratory conditions. Second, the humidity near the surface is near saturation in natural conditions, whereas a less humid environment was adopted in the laboratory. Therefore, the laboratory data were adjusted 5 m/s lower to obtain more realistic figures.

Lai and Shemdin (1974) measured the height distribution of the drops and found no drops above the height Z_{od}, depending on the windspeed. However, these measurements are difficult to apply for the natural case because of the differences in surface roughness and humidity. Furthermore, the freezing factor may be different for the higher flying drops because evaporation may increase salt concentration in the drops.

The effect of fetch on the flux droplets and Z_{od} was studied by Wang and Street (1978). They indicated in their Figure 7 a rather parabolic increase of Z_{od} with increase in fetch. No

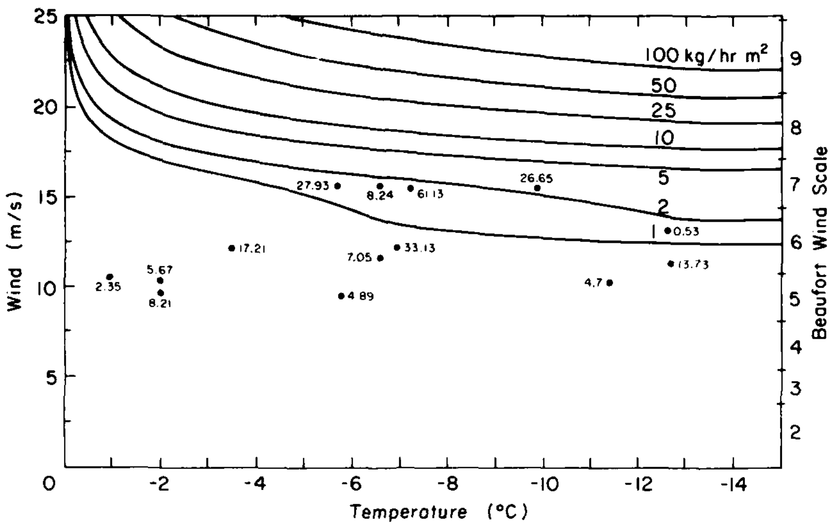

Figure 4. Ice accumulation rate R as a function of temperature and windspeed. Numbers next to data points indicate values (kg/m^2hr) measured onboard ships (Ono 1964).

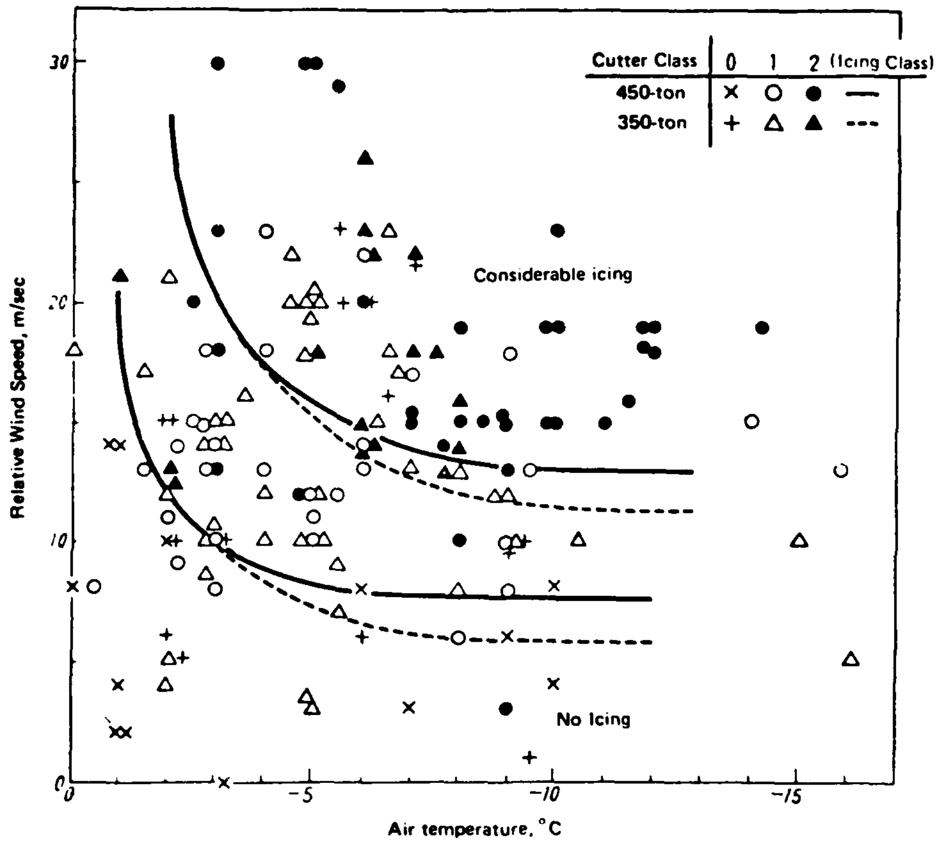

Figure 5. Effect of air temperature and relative windspeed on ice accretion class (after Tabata 1969) (copyright T. Tabata; reprinted by permission).

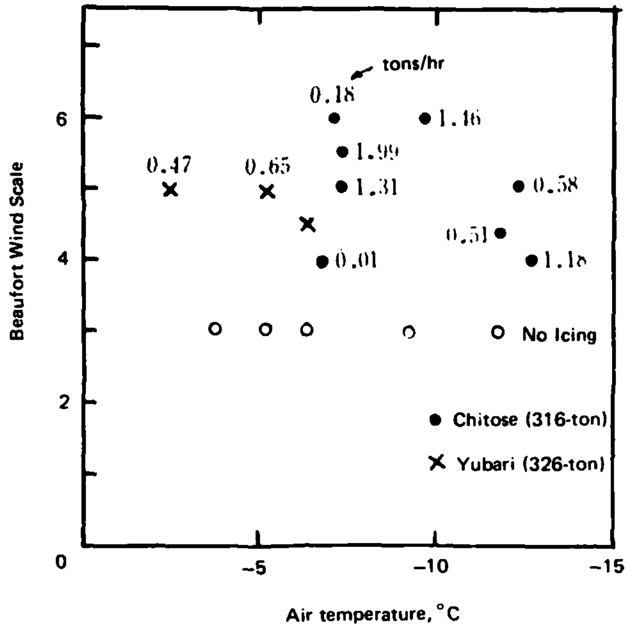

Figure 6. Total ice accumulation rate measured on the Japanese cutters Chitose *and* Yuburi (*after Tabata et al. 1963*) (*copyright T. Tabata; reprinted by permission*).

saturation was attained within their limit of fetch (12.5 m). Because no appreciable difference in droplet size distribution can be observed in their Figure 6, which shows a droplet histogram for different fetches, mass flux at the fixed height increases as the fetch increases. It is difficult to extrapolate their experimental results into the natural condition. However, a 5-m/s difference in windspeed, corresponding to the difference in mass flux between natural observations and laboratory experiments, seems reasonable.

Neglected factors such as sea spray flux, windspeed and water temperature may be responsible for the wide scatter of the data points in Figure 1. Actually, most of the low sea spray flux data, as indicated in this figure, lie above the regression line, indicating that more factors have to be taken into account. However, limitations in the available data precluded further refinement.

Considering these differences in icing conditions, especially differences in the drop generation mechanisms, direct comparison between the data obtained from ship observations and from the theoretical calculations described here for stationary structures may be inappropriate. The general trend found in Figures 5 and 6, obtained from ship observations made by Tabata (1969) and Tabata et al. (1963), shows strong similarities between their data and the theoretical results shown in Figure 4, however. Those similarities seem to indicate that the approach of the present analysis is in the correct direction, but that there is a need for more accurate icing data from stationary structures to compare with this particular analysis.

LITERATURE CITED

Lai, R.J. and O.H. Shemdin (1974) Generation of spray over water. *Journal of Geophysical Research,* **79**(21): 3055–3063.

Monahan, E.C. (1968) Sea spray as a function of low-elevation wind speed. *Journal of Geophysical Research,* **73**: 1127–1137.

Ono, N. (1964) Studies of ice accumulation on ships, II. *Low Temperature Science,* Series A, part 22, pp. 171–181.

Tabata, T., S. Iwata and N. Ono (1963) Studies of ice accumulation on ships, I. *Low Temperature Science,* Series A, part 21, pp. 173–221.

Tabata, T. (1969) Studies of ice accumulation on ships, III. *Low Temperature Science,* Series A, part 27, pp. 337–349.

Toba, Y. (1961) Drop production by bursting air bubbles on the sea surface, 3. Study by use of wind flume. *Memorial College of Science, University of Kyoto,* Series A(20): 313–344.

Wang, C.S. and R. Street (1978) Transfers across an air–water interface at high wind speeds: The effect of spray. *Journal of Geophysical Research,* **83**: 2959–2969.

A facsimile catalog card in Library of Congress MARC format is reproduced below.

Itagaki, Kazuhiko
Icing rate on stationary structures under marine conditions / by Kazuhiko Itagaki. Hanover, N.H.: Cold Regions Research and Engineering Laboratory; Springfield, Va.: available from National Technical Information Service, 1984.
ii, 13 p., illus.; 28 cm. (CRREL Report 84-12.)
Prepared for Office of the Chief of Engineers by Corps of Engineers, U.S. Army Cold Regions Research and Engineering Laboratory under DA Project 4A1611 02AT24.
Bibliography: p. 8.
1. Icing. 2. Ice formation. 3. Offshore drilling. 4. Offshore structures. 5. Ships. 6. Ship icing. I. United States. Army. Corps of Engineers. II. Cold Regions Research and Engineering Laboratory, Hanover, N.H. III. Series: CRREL Report 84-12.

END

FILMED

10-84

DTIC